引用格式:CHEN ChunYu, DING Xuan, LI ShouChuan, et al. Microwave-assisted sol-gel synthesis of hydroxyapatite nanoparticles [J]. Journal of Beijing University of Chemical Technology (Natural Science), 2019,46(3):7-15.

Microwave-assisted sol-gel synthesis of hydroxyapatite nanoparticles

CHEN ChunYu[1] DING Xuan[2] LI ShouChuan[1] SUN BaoChang[1] LV ShanShan[1]*

(1. State Key Laboratory of Organic-Inorganic Composite Materials, College of Chemical Engineering, Beijing University of Chemical Technology, Beijing 100029;
2. State Key Laboratory of Analytical Chemistry for Life Science, Nanjing University, Nanjing 210023, China)

Abstract: A rapid sol-gel method for preparing hydroxyapatite nanoparticles (nHAP) has been developed. Three different sets of experimental conditions, in terms of solvents (water and ethanol), synthesis temperatures (25, 40 and 60℃), and microwave irradiation (on and off) were explored. Crystal phase composition, functional groups and morphology of the products were characterized by thermogravimetric analysis (TGA), X-ray diffraction (XRD), Fourier transform infrared spectroscopy (FT-IR), scanning electron microscopy (SEM) and transmission electron microscopy (TEM). The solvent and temperature were optimized based on product properties. Most importantly, the microwave-assisted method (with little to no ageing necessary) was much faster than the conventional methods (with slow ageing processes needing from hours to days), while affording pure nHAP with virtually identical morphological and structural properties. This study represents a practical application of the powerful microwave technique in synthesis of nHAP, offering guidance on the selection of optimum experiment conditions.

Key words: hydroxyapatite; sol-gel; temperature; microwave
PACS: TQ126.3 **DOI**: 10.13543/j.bhxbzr.2019.03.002

Introduction

Hydroxyapatite (HAP, chemically represented as $Ca_{10}(PO_4)_6(OH)_2$) is the major constituent (70% - 90%) of biological apatite in vertebrates[1]. Because of its close chemical and crystallographic structure resemblance to natural bones and teeth, along with its good bioaffinity, superior bioresorption and enhancement of osteoconductivity, HAP is one of the most attractive and frequently used calcium phosphate-based biomaterials in the form of restorative, grafting, and coating materials in clinical applications such as dental and orthopedic implants[1-2]. Due to extensive use of HAP, synthetic HAP, especially nano-hydroxyapatite (nHAP) is of great interest. Various methods have been developed for the synthesis of HAP nanostructures, including dry processes (such as mechanochemical synthesis[3-4] and combustion synthesis[5-6]), and wet chemistry techniques (such as precipitation methods[7-8], sol-gel processes[1-2], hydrothermal processes[9-10], emulsion systems[11-13], ultrasonic techniques[14] and high gravity methods[15]). Among them, sol-gel processes, one of the most economic and environmentally friendly approaches, have attracted much attention because of its well-known inherent advantages, including homogeneous molecular mixing and thereby homogeneous chemical composition and high product purity, low processing temperature, ability to produce fine-grain nano-sized particles, and tremendous flexibility to generate powders, bulk amorphous monolithic solids and thin films[16-17]. Howev-

Received: 2018-08-27
Foundation Items: National Key Research Program of China (2016YFA0201700/2016YFA02017001); National Natural Science Foundation of China (31400813)
First Author: female, born in 1994, postgraduate
* Corresponding Author
E-mail: lvshanshan@mail.buct.edu.cn

er, due to slow reactions between calcium (Ca) and phosphorus (P) precursors in the sol phase, the sol – gel preparation processes commonly reported in literature are time-consuming that usually need a long period of time (≥24 h in the order of several days even over a week) to complete the ageing and drying process[2], which limits the production application of synthetic HAP at industrial scale.

Microwave(MW) is electromagnetic wave whose frequency range falls from 300 to 300 000 MHz. The electromagnetic energy induces motion of molecular dipole moments inside dielectric materials, and generates heat internally and simultaneously both at the core and the surface of materials. In conventional heating methods, the external heating source transfers energy radiatively into materials[17]. Hence, MW-assisted methods offer several distinct advantages including rapid heating, throughout volume heating, shorter reaction time, efficient energy transformation and excellent reproducibility[18]. Recently, MW-assisted synthesis of nHAP has become a fast-growing research area[18-19]. There have been several reports demonstrating MW-assisted synthesis of nHAP for various applications[20-21]. For example, MW-precipitation methods, MW-sintering methods and MW-hydrothermal methods have been proved to be successful in a rapid synthesis of HAP[18-19,22].

The sol – gel process may also become faster with microwave assistance. However, to our knowledge, there have been few reports on combining these two techniques[23]. In this study, we reported for the first time a simple MW-assisted sol – gel method (MW–SG) for rapid (with little or no ageing process) synthesis of nHAP from calcium nitrate tetrahydrate and phosphoric pentoxide. In order to clearly understand the process of synthesis reaction, the effect of different parameters, such as solvent, temperature and microwave, were investigated. A conventional sol – gel process was also studied for comparison purpose. The MW-assisted sol – gel method was found to be much quicker than that used in the conventional ethanol based sol – gel nHAP synthesis, while their products were chemically identical.

1 Experimental

1.1 Materials and equipment

Calcium nitrate tetrahydrate ($Ca(NO_3)_2 \cdot 4H_2O$), phosphoric pentoxide (P_2O_5), absolute ethanol (CH_3CH_2OH) and ammonia hydroxide (NH_4OH) and all other reagents were purchased from Sinopharm Chemical Reagent Beijing Co. Ltd., and were analytical reagent grade and used without further purification.

All microwave-assisted reactions were carried out in a microwave-assisted reactor (MCR – 3, Shanghai Purdue Biochemical Technology Co., Ltd., Shanghai). The power source to generate microwave at a frequency of 2.45 GHz is installed because it has suitable penetration depth to interact with chemical compounds. This system is operated at 50 Hz and a maximum power of 800 W, and the power could be tuned from 0 to 100% and controlled by temperature from 40 ℃ to a maximum of 250 ℃.

1.2 Preparation of hydroxyapatite

Calcium nitrate tetrahydrate ($Ca(NO_3)_2 \cdot 4H_2O$) and phosphoric pentoxide (P_2O_5) dissolved in absolute ethanol were used as the starting precursors for calcium and phosphorous, respectively. The calcium solution was stirred at room temperature and the phosphate solution was added dropwisely. The reactants were mixed according to the stoichiometric hydroxyapatite molar ratio ($n_{Ca}/n_P = 1.67$). Ammonium hydroxide (NH_4OH) was used to adjust the pH of the solution to 8. The obtained mixture was heated to the required temperature (25, 40 and 60 ℃) in a conventional water bath reactor or in a microwave reactor (2.45 GHz, 800 W) for 10 min with vigorously stirring. A white viscous solution was obtained, and then aged at room temperature for different time periods up to 48 h. The white gel transformed from the solution was filtered and washed repeatedly using distilled water. The filtered gel-like cake was dried overnight in air oven at above 80 ℃ (labeled as precursor). The dried precursor was then calcined at 600 ℃ for 2 h in air using a muffle furnace to produce hydroxyapatite.

1.3 Characterization of hydroxyapatite

1.3.1 Thermal gravimetric analysis (TGA)

TGA was conducted under an air atmosphere in a NETZSCH STA 449C apparatus (Shimadzu, Japan) with a 10 ℃/min ramp between 20 and 800 ℃. Approximately 4 mg of sample was ground with a mortar and pestle and then placed in a ceramics sample pan for analysis.

1.3.2 X-ray diffraction analysis (XRD)

The crystalline phases of the samples were examined by XRD analysis (XRD－6000, Shimadzu, Japan), using Cu Kα radiation ($\lambda = 0.15406$ nm) in a 2θ range of 5° to 90° at a scan rate of 5 (°)/min. Powder samples were densely packed in an aluminum holder. The experiments were operated at a voltage and current setting of 40 kV and 30 mA, respectively. Spectrum analysis software MDI Jade V 5.0.37 was used. Crystallographic identification of the XRD patterns was accomplished by comparing with standard data compiled by the International Centre for Diffraction Data (ICDD).

1.3.3 Fourier transform infrared spectroscopy (FT-IR)

Infrared transmittance spectra of the samples were obtained using a Fourier transform infrared spectrometer (Bruker Optics VERTEX70, USA) in the transmission mode in the range of 400－4 000 cm^{-1} with a resolution of 4 cm^{-1}. Pellets for FT-IR were prepared by mixing the sample with potassium bromide (KBr) in a mass ratio of 1∶100 to form a homogeneous mixture, and compressed at 10 MPa to form disks at room temperature.

1.3.4 Scanning electron microscopy (SEM)

For SEM experiments, the samples were carefully fixed on aluminum stubs and then coated by 5 nm of gold, and measurements were performed on a TESCAN MAIA3 microscope (TESCAN, Czech).

1.3.5 Transmission electron microscopy (TEM)

TEM experiments were performed on an HT7700 microscope (Hitachi, Japan). The samples for TEM characterization were prepared by dissolving in absolute ethanol and evaporating a droplet of dispersion on a Cu grid. The morphology and size of the samples were investigated. Diameters and lengths and corresponding distributions were derived from the TEM images using ImageJ (NIH, USA).

2 Results and discussion

2.1 The sol－gel process

Various methods for microwave-assisted (MW) synthesis of nano-hydroxyapatite (nHAP) have extensively investigated the effect of MW on the properties of nHAP, such as Ca/P ratio, particle size and shape, phase and crystal structure, morphology and biological properties. The aim of this work was to evaluate the MW-assisted method as a synergetic strategy for sol－gel synthesis of nHAP. The reaction involved in the present study can be expressed as follows:

$$10Ca(NO_3)_2 \cdot 4H_2O + 3P_2O_5 + 20NH_4OH \longrightarrow Ca_{10}(PO_4)_6(OH)_2 + 20NH_4NO_3 + 49H_2O.$$

Figure 1 showed representative photographs of the asprepared products in the form of gels during the sol－gel method.

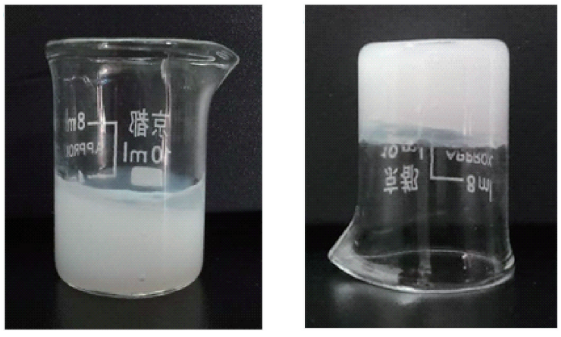

Fig. 1　Representative photographs of the asprepared products of the sol－gel process

2.2 Solvent effect

It has been reported that a typical aqueous sol－gel synthesis of HAP often requires ageing and drying periods up to a week or more, while non-aqueous ethanol-based process can be significantly faster[2]. For comparison, the sol－gel processes were carried out in both water and ethanol in this study. After drying, the precursor was evaluated by thermal gravimetric analysis to investigate its thermal stability (Figure 2(a)) and optimized sintering temperature. For the aqueous sol－gel process, the first stage of weight loss was at $T \leqslant$ 250 ℃ due to evaporation of absorbed and lattice water;

the second one was at 250 ℃ ≤T≤320 ℃ and the third one was at 320 ℃ ≤T≤450 ℃. For the ethanol-based sol－gel process, the first one was at T≤280 ℃ due to lattice water and ethanol evaporation, and the second one was at 280 ℃ ≤T≤600 ℃ due to decomposition and burnout of ethanol and crystallization of nHAP. Beyond 600 ℃, there was no significant change in weight loss representing stable nHAP. It has been mentioned that the decomposition/degradation temperature of nHAP was in the range of 600－900 ℃[2] and that HAP transformed into other phases during heating up to 1 200 ℃[24]. As a result, the calcination temperature was set as 600 ℃ in the present study.

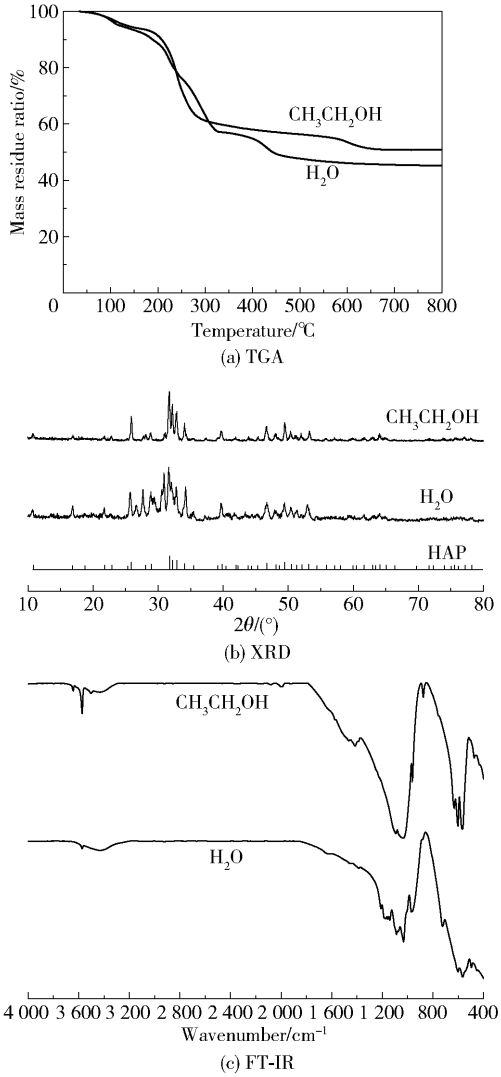

Fig. 2 TGA, XRD and FT-IR analysis results showing the effect of different solvents on the structure of the products

In order to determine any potential preferential crystalline orientation produced by the variation of reaction solvents, X-ray powder diffraction was used to identify the crystalline phases of sintered products at 600 ℃. The XRD patterns were shown in Figure 2(b). The XRD patterns of product prepared by the aqueous sol－gel process exhibited characteristic patterns of nHAP. But low resolution and intensity suggested poorly crystalline single phase of HAP. The XRD patterns of product prepared by the ethanol-based process showed increase in resolution and intensity at (0 0 2) and (2 1 1) planes. Again there was no crystalline phase other than HAP. In addition, FT-IR spectroscopy was used to confirm the molecular structure and functional groups in the nHAP. Figure 2(c) showed all bands corresponding to nHAP. Bands at 600 and 1 020 cm^{-1} represented the ν4 and ν3 bending vibrations of PO_4^{3-}. Bands at 3 570 and 630 cm^{-1} were attributed to the characteristic ν3 and νL OH^- stretching of the nHAP lattice[25]. Further structural analysis of the synthesized nHAP was characterized using both scanning electron microscopy and transmission electron microscopy (Figure 3 and 4). The nHAP synthesized through the ethanol-based sol－gel process exhibited nano-sized morphology, while that of the aqueous sol－gel process was mainly amorphous with no distinct edges (Figure 3(a)、(b) and Figure 4(a)、(b)). This result agreed well with the above XRD results. In summary, different reaction solvents affected the crystalline properties of nHAP product, and it was found that ethanol was a better solvent for the sol－gel method. Moreover, most reports in literature indicated that the sol－gel derived HAP was always accompanied by secondary phase of calcium oxide, which might not be favorable for certain applications[26]. In contrast, this study represented an ethanol-based sol－gel synthesis of pure phase nHAP.

2.3 Temperature effect

It has been reported that temperature affects the morphology, crystallinity and stoichiometry of nHAP precipitation[27]. The sol－gel processes were carried out at 25, 40 and 60 ℃, respectively. The TGA traces were shown in Figure 5(a). For precursors produced at 25 and 40 ℃, there were three major weight loss sta-

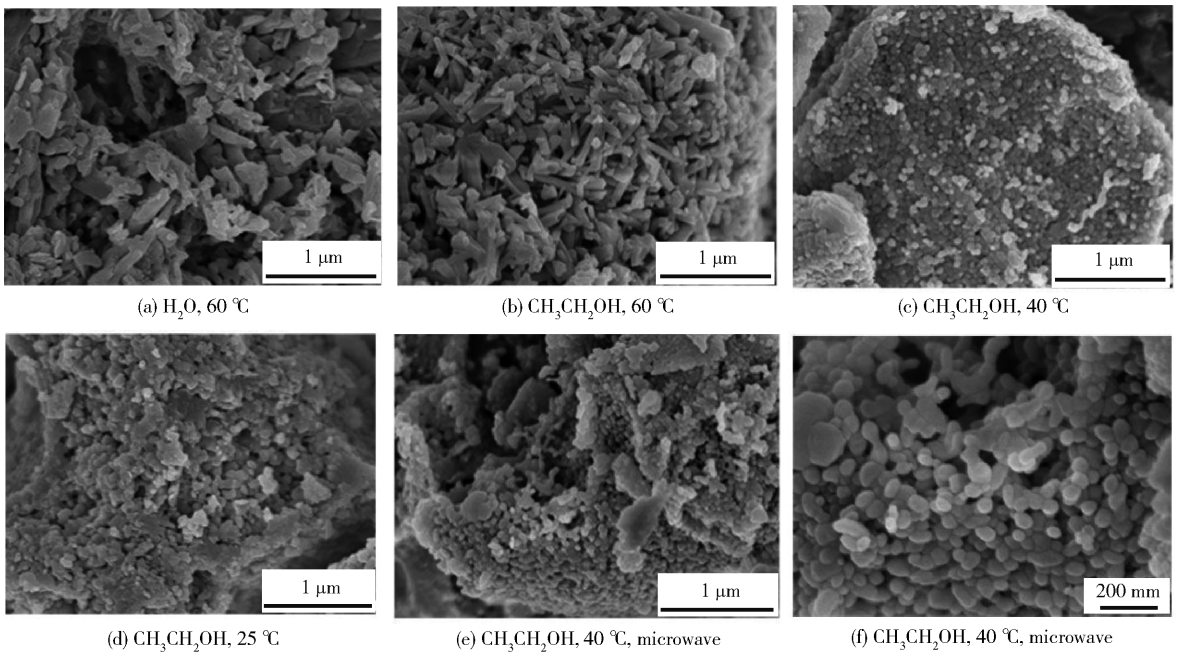

(a) H_2O, 60 ℃　(b) CH_3CH_2OH, 60 ℃　(c) CH_3CH_2OH, 40 ℃

(d) CH_3CH_2OH, 25 ℃　(e) CH_3CH_2OH, 40 ℃, microwave　(f) CH_3CH_2OH, 40 ℃, microwave

Fig. 3　Representative SEM images of hydroxyapatite nanoparticles prepared under different reaction conditions

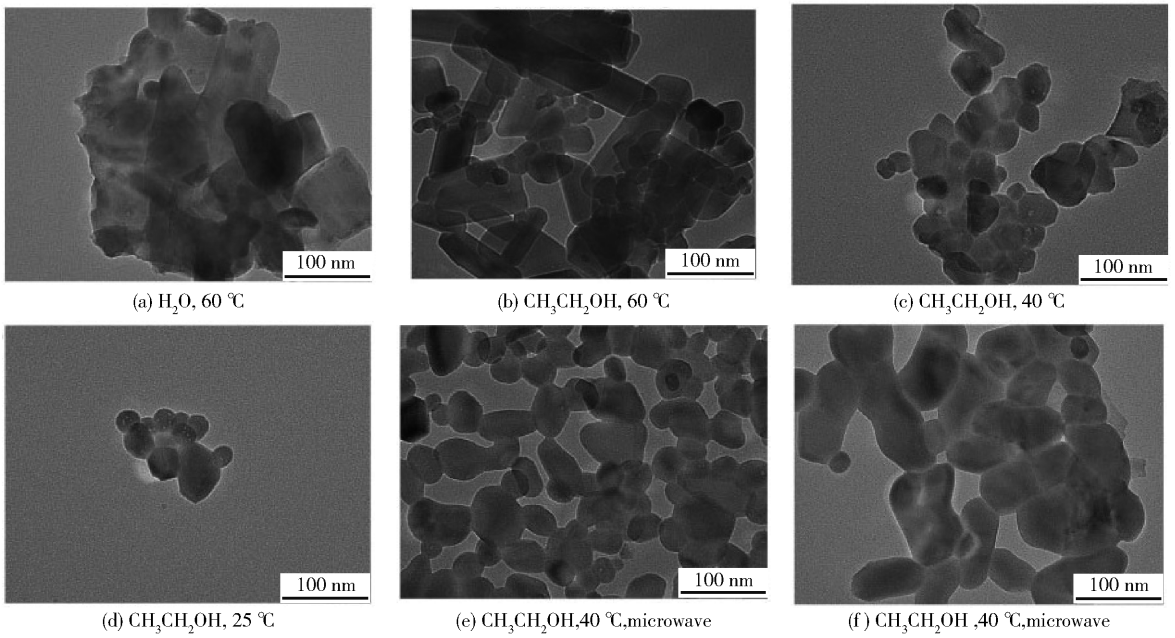

(a) H_2O, 60 ℃　(b) CH_3CH_2OH, 60 ℃　(c) CH_3CH_2OH, 40 ℃

(d) CH_3CH_2OH, 25 ℃　(e) CH_3CH_2OH,40 ℃,microwave　(f) CH_3CH_2OH ,40 ℃,microwave

Fig. 4　Representative TEM images of hydroxyapatite nanoparticles prepared under different reaction conditions

ges, while two stages for 60 ℃. As for the crystalline phase, the XRD patterns were similar in all three cases, showing single crystalline phase HAP (Figure 5 (b)). The FT-IR spectra in Figure 5(c) showed the characteristic bands of nHAP. Besides, the spectra of all the samples showed a sharp and strong band at about 3 570 cm^{-1} and a weak broad band ranging from 3 200 to 3 600 cm^{-1}. The 3 570 cm^{-1} around band corresponded to the OH^- group, and the broad band corresponded to the strongly adsorbed/bound water (stretching mode) in the structure. Even though the crystal phases were similar in all ethanol-based sol-gel processes, morphological properties might differ due to different processing temperature.

More detailed structural analysis by SEM and TEM was performed. Figure 3(b) - (d) and Figure 4

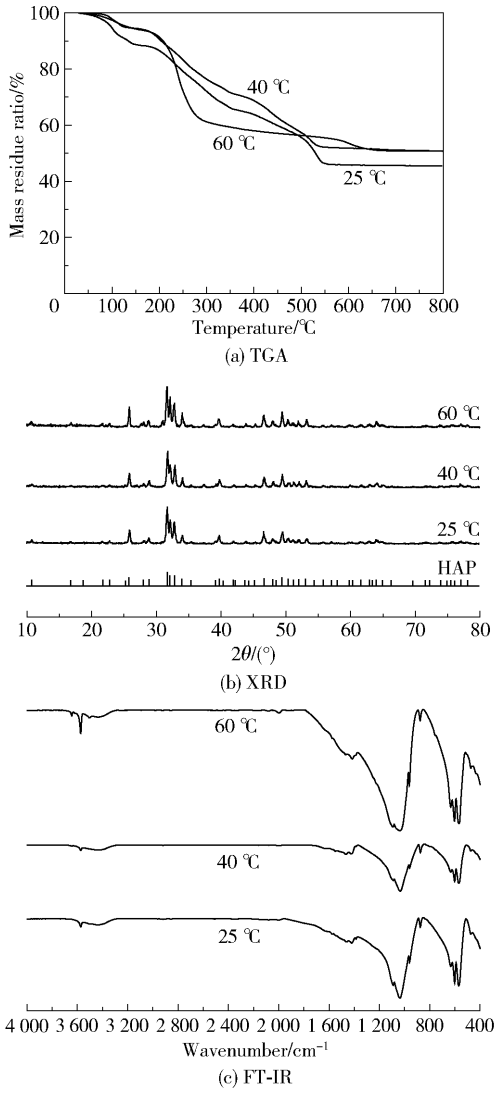

Fig. 5 TGA, XRD and FT-IR analysis results showing the effect of the temperature on the structure of the products

(b) – (d) showed representative images of the nHAP produced at 25, 40 and 60 ℃, respectively. It was observed that the particle sizes of the nHAP increased along with the reaction temperature. It can be seen that the nHAP prepared at 60 ℃ was much larger than that at 25 ℃. More specially, the HAP prepared at 25 ℃ was mainly nanosphere-shaped (Figure 3(d) and 4(d)), while that prepared at 40 ℃ was nanoellipse-shaped (Figure 3(c) and 4(c)) and that prepared at 60 ℃ was a mixture of nanoellipse-shaped and nanorod-like structures (Figure 3(b) and 4(b)). This trend was consistent with the previous report that the increase of reaction temperature favored formation of calcium phosphate with larger particle size[20]. In summary, temperature did not affect the crystalline phase (XRD), slightly affected the functional groups (FT-IR), but did affect thermal stability of the precursors (TGA) and nanostructure morphology (SEM and TEM) of the final nHAP.

2.4 Microwave effect

Nearly all types of thermally driven chemical reactions could be accelerated by microwave irradiation. To evaluate the effect of MW on the sol – gel process, reactions were carried out with and without MW. The reaction temperature was set as 40 ℃ for two reasons: (1) SEM and TEM results (Figure 3(c) and 4(c)) indicated that the particle size distribution of nHAP at 40 ℃ was the most uniform and least agglomeration; (2) 40 ℃ was the lowest temperature limit of the MW reactor used in the present study. After 10 min-heating at 40 ℃, 5 min-ageing was taken for the MW-assisted sol – gel process, while 48h-ageing was taken for the conventional heating method. It is noteworthy that, in most previous reports, the reaction temperature was not mentioned as there were no temperature measuring tools in domestic MW ovens, which lacked control, reproducibility and safety[18 – 20]. A commercially available single-mode microwave reactor was employed in this study which was installed with built-in magnetic stirring, temperature and pressure sensors, power control and feedback control. This microwave system enabled easy, repeatable, reliable and effective control of the reaction temperature.

From Figure 6, it can be seen that there were no significant differences between the products synthesized via the MW-assisted sol – gel process and that from the conventional heating method. Meanwhile, the maturation degree of the resultant precipitate revealed that the conventional method required a longer time to approach the thermodynamic equilibrium than the MW-assisted heating. The reaction of $Ca(NO_3)_2 \cdot 4H_2O$ with P_2O_5 in ethanol resulted in the formation of a gel. Whether the resultant gel was transparent or translucent depended on the precipitate concentration. As shown in Figure 7, the gels resulted from MW-assisted heating without any ageing stages were more translucent than that

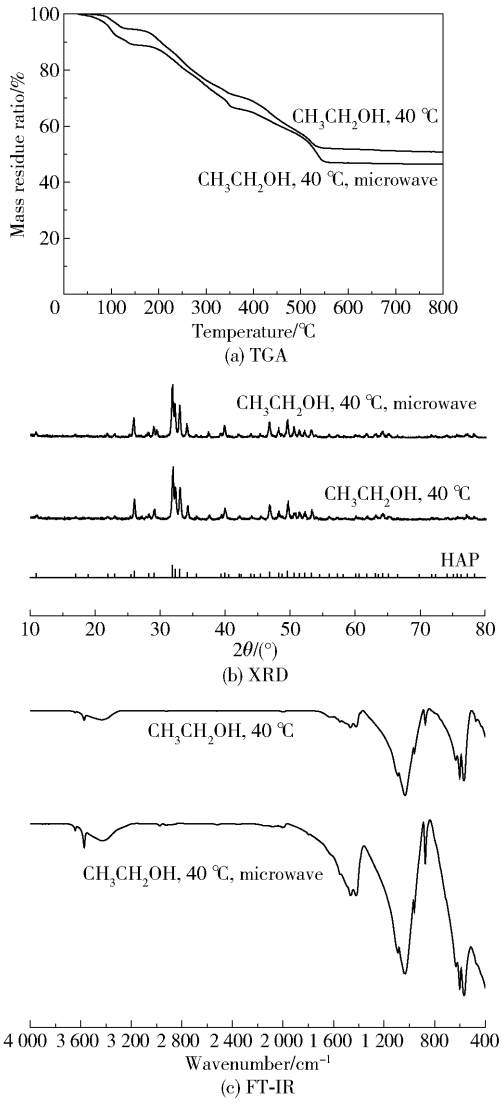

Fig. 6　The TGA, XRD and FT-IR analysis results showing the effect of microwave irradiation on the structure of the products at 40 ℃ (the lowest temperature limited by the microwave reactor)

from the conventional method even after 48 h-ageing. These results highlighted the speediness of the MW-assisted sol－gel method proposed in the present work, which could potentially avoid the ageing process entirely. The short reaction time was consistent with previously reported MW-assisted synthesis methods of nHAP[18－19, 22]. This could be attributed to the interaction of the MW with the dielectric nHAP and solvent molecules at the molecular level. The MW energy raised local temperature, and consequently reduced the maturation time required for formation of nHAP phase[28]. Instead of spending hours or even days syn-

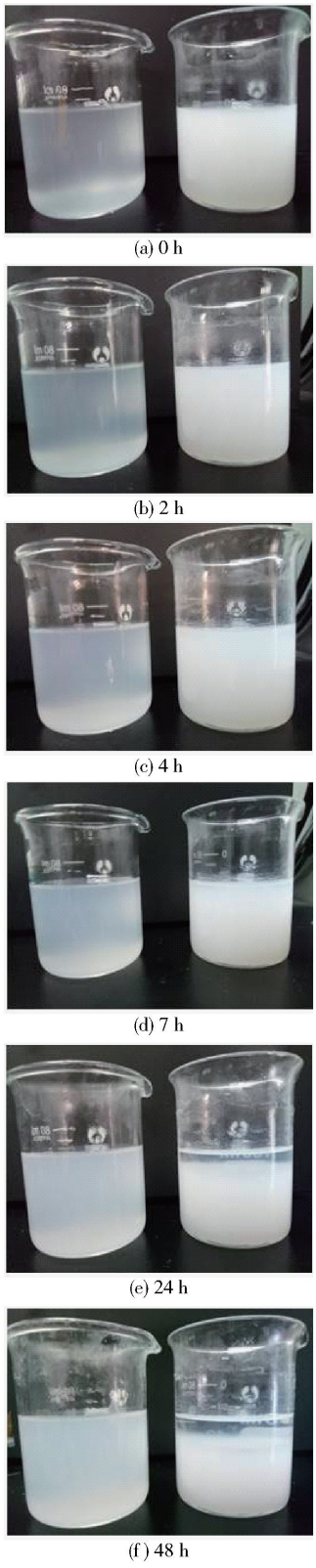

Fig. 7　Photographs of sol－gel materials aged for different time periods showing products obtained from conventional heating (left) and microwave-assisted heating (right)

thesizing nHAP, the same sol – gel reaction could be accomplished in minutes. Further structural characterization using SEM and TEM (Figure 3(e) – (f) and Figure 4(e) – (f)) revealed nanoellipse-shaped morphologies with no obvious differences, suggesting that the MW has no significant influence on the morphology of nHAP. In previous studies, via MW irradiation, Lak et al.[29] reported the synthesis of rod-like hydroxyapatite, Liu et al.[30] reported the synthesis of needle-like hydroxyapatite. But in both above cases the nanostructures showed poor crystallinity, and the morphology could not be well controlled. In the present study, the use of sol – gel synthesis in combination with microwave heating made it possible to obtain nHAP with high crystallinity and uniform morphology.

3 Conclusions

We developed a new microwave-assisted sol – gel method with obviously higher efficiency over conventional methods for preparing hydroxyapatite nanoparticles (nHAP). The innovative fast process required little or no aging while the conventional method involved a 48h-aging period. The morphological and structural properties of nHAP were investigated. It was found that ethanol was a better solvent for the sol – gel method in producing nHAP with high crystalline pure phase, and that the particle size of the nHAP increased along with the reaction temperature. In addition, the microwave irradiation did not affect the morphological or structural properties of nHAP. Therefore, the microwave-assisted sol – gel method has great potential as a rapid technique to prepare nHAP, and the fast production broadens the scope of nHAP for future academic and industrial applications.

References:

[1] WANG F, LI M S, LU Y P, et al. A simple sol-gel technique for preparing hydroxyapatite nanopowders [J]. Materials Letters, 2005, 59(8): 916–919.

[2] FATHI M H, HANIFI A. Evaluation and characterization of nanostructure hydroxyapatite powder prepared by simple sol-gel method [J]. Materials Letters, 2007, 61(18): 3978–3983.

[3] KIM W, ZHANG Q W, SAITO F. Mechanochemical synthesis of hydroxyapatite from $Ca(OH)_2 - P_2O_5$ and $CaO - Ca(OH)_2 - P_2O_5$ mixtures [J]. Journal of Materials Science, 2000, 35(21): 5401–5405.

[4] NASIRI-TABRIZI B, HONARMANDI P, EBRAHIMI-KAHRIZSANGI R, et al. Synthesis of nanosize single-crystal hydroxyapatite via mechanochemical method [J]. Materials Letters, 2009, 63(5): 543–546.

[5] TAS A C. Combustion synthesis of calcium phosphate bioceramic powders [J]. Journal of the European Ceramic Society, 2000, 20(14): 2389–2394.

[6] VARMA H K, KALKURA S N, SIVAKUMAR R. Polymeric precursor route for the preparation of calcium phosphate compounds [J]. Ceramics International, 1998, 24(6): 467–470.

[7] PRETTO M, COSTA A L, LANDI E, et al. Dispersing behavior of hydroxyapatite powders produced by wet-chemical synthesis[J]. Journal of the American Ceramic Society, 2003, 86(9): 1534–1539.

[8] ZHANG H Q, WANG Y F, YAN Y H, et al. Precipitation of biocompatible hydroxyapatite whiskers from moderately acid solution [J]. Ceramics International, 2003, 29(4): 413–418.

[9] LIN K L, CHANG J, CHENG R M, et al. Hydrothermal microemulsion synthesis of stoichiometric single crystal hydroxyapatite nanorods with mono-dispersion and narrow-size distribution [J]. Materials Letters, 2007, 61(8): 1683–1687.

[10] LIU H S, CHIN T S, LAI L S, et al. Hydroxyapatite synthesized by a simplified hydrothermal method [J]. Ceramics International, 1997, 23(1): 19–25.

[11] SHUM H C, BANDYOPADHYAY A, BOSE S, et al. Double emulsion droplets as microreactors for synthesis of mesoporous hydroxyapatite [J]. Chemistry of Materials, 2009, 21(22): 5548–5555.

[12] GUO G S, SUN Y X, WANG Z H, et al. Preparation of hydroxyapatite nanoparticles by reverse microemulsion [J]. Ceramics International, 2005, 31(6): 869–872.

[13] WU Y Q, HENCH L L, DU J, et al. Preparation of hydroxyapatite fibers by electrospinning technique [J]. Journal of the American Ceramic Society, 2004, 87(10): 1988–1991.

[14] WAKIYA N, YAMASAKI M, ADACHI T, et al. Preparation of hydroxyapatite-ferrite composite particles by ultrasonic spray pyrolysis [J]. Materials Science and Engineering B, 2010, 173(1/2/3): 195–198.

[15] NATHANAEL A J, HONG S I, MANGALARAJ D, et al. Large scale synthesis of hydroxyapatite nanospheres by

high gravity method [J]. Chemical Engineering Journal, 2011, 173(3): 846-854.

[16] DESHPANDE S B, KHOLLAM Y B, BHORASKAR S V, et al. Synthesis and characterization of microwave-hydrothermally derived $Ba_{1-x}Sr_xTiO_3$ powders [J]. Materials Letters, 2005, 59(2): 293-296.

[17] BEN-NISSAN B, MILEV A, VAGO R. Morphology of sol-gel derived nano-coated coralline hydroxyapatite [J]. Biomaterials, 2004, 25(20): 4971-4975.

[18] KALITA S J, VERMA S. Nanocrystalline hydroxyapatite bioceramic using microwave radiation: synthesis and characterization [J]. Materials Science and Engineering C, 2010, 30(2): 295-303.

[19] PARHI P, RAMANAN A, RAY A R. A convenient route for the synthesis of hydroxyapatite through a novel microwave-mediated metathesis reaction [J]. Materials Letters, 2004, 58(27): 3610-3612.

[20] HASSAN M N, MAHMOUD M M, El-FATTAH A A, et al. Microwave-assisted preparation of nano-hydroxyapatite for bone substitutes [J]. Ceramics International, 2016, 42(3): 3725-3744.

[21] DEMIRTAŞ T T, KAYNAK G, GÜMÜŞDERELIOĞLU M. Bone-like hydroxyapatite precipitated from 10× SBF-like solution by microwave irradiation [J]. Materials Science and Engineering C, 2015, 49: 713-719.

[22] MÉNDEZ-LOZANO N, VELÁZQUEZ-CASTILLO R, RIVERA-MUÑOZ E M, et al. Crystal growth and structural analysis of hydroxyapatite nanofibers synthesized by the hydrothermal microwave-assisted method [J]. Ceramics International, 2017, 43(1): 451-457.

[23] BEN-ARFA B A E, SALVADO I M M, FERREIRA J M F, et al. Novel route for rapid sol-gel synthesis of hydroxyapatite, avoiding ageing and using fast drying with a 50-fold to 200-fold reduction in process time [J]. Materials Science and Engineering C, 2017, 70: 796-804.

[24] RAYNAUD S, CHAMPION E, BERNACHE-ASSOLLANT D, et al. Calcium phosphate apatites with variable Ca/P atomic ratio I. Synthesis, characterisation and thermal stability of powders [J]. Biomaterials, 2002, 23(4): 1065-1072.

[25] WANG Y J, CHEN J D, WEI K, et al. Surfactant-assisted synthesis of hydroxyapatite particles [J]. Materials Letters, 2006, 60(27): 3227-3231.

[26] KURIAKOSE T A, KALKURA S N, PALANICHAMY M, et al. Synthesis of stoichiometric nano crystalline hydroxyapatite by ethanol-based sol-gel technique at low temperature [J]. Journal of Crystal Growth, 2004, 263(1/2/3/4): 517-523.

[27] LIU Y K, WANG W Z, ZHAN Y J, et al. A simple route to hydroxyapatite nanofibers [J]. Materials Letters, 2002, 56(4): 496-501.

[28] KATSUKI H, FURUTA S, KOMARNENI S. Microwave-versus conventional-hydrothermal synthesis of hydroxyapatite crystals from gypsum [J]. Journal of the American Ceramic Society, 1999, 82(8): 2257-2259.

[29] LAK A, MAZLOUMI M, MOHAJERANI M S, et al. Rapid formation of mono-dispersed hydroxyapatite nanorods with narrow-size distribution via microwave irradiation [J]. Journal of the American Ceramic Society, 2008, 91(11): 3580-3584.

[30] LIU J B, LI K W, WANG H, et al. Self-assembly of hydroxyapatite nanostructures by microwave irradiation [J]. Nanotechnology, 2005, 16(1): 82-87.

(责任编辑:吴万玲)